# GRAPHITE AND XENON BEHAVIOR AND THEIR INFLUENCE ON MOLTEN-SALT REACTOR DESIGN

DUNLAP SCOTT and W. P. EATHERLY *Oak Ridge National Laboratory, Nuclear Division, Oak Ridge, Tennessee 37830*

REACTORS

**KEYWORDS:** *molten-salt reactors, breeder reactors, radiation effects, temperature, graphite moderator, stresses, porosity, xenon-135, poisoning, helium, bubbles, design, economics, reactor core, MSBR*

Received August 4, 1969
Revised October 2, 1969

*Existing data on dimensional changes in graphite have been fitted to parabolic temperature-sensitive curves. From these, the graphite life, radiation-induced stresses, and permissible geometries have been calculated. It is concluded existing materials can be utilized in a molten-salt reactor which has a core graphite life of about four years, without serious cost penalty.*

*Fission product xenon can be removed by sparging the fuel salt with helium bubbles and removing them after enrichment. With reasonable values of salt-to-bubble transfer coefficient and graphite permeability, the penalty to breeding ratio can be reduced to <0.5%.*

## INTRODUCTION

One of the attractive aspects of the molten-salt reactor concept is that even the most stringent of the present materials or process limitations permit reactor designs having acceptable economic performance. In this paper we consider, as examples, the effects of finite graphite lifetime and xenon poisoning on MSBR design. Finite graphite lifetime implies periodic replacement of the graphite; neutron economy requires the removal of the bulk of $^{135}Xe$ from the core to keep the xenon poison fraction below the target value of $\frac{1}{2}\%$.

The major economic penalty associated with graphite replacement would be the load factor penalty associated with taking the reactor off-stream. This cost can be circumvented by assuring that the graphite will maintain its integrity for at least the time interval between normal turbine maintenance requirements; i.e., the downtime required for scheduled maintenance should coincide with that for graphite replacement. Hence, to avoid load-factor penalties associated with graphite replacement, we have set as a minimum requirement that the graphite have a life of two years; at the same time, a longer life would be desirable and consistent with the power industry's objective of increasing the time interval between turbine maintenance operations. Thus, in the reference design the reactor performance is constrained to yield a graphite life of about four years, and this paper points out the basis for that value.

The removal of $^{135}Xe$ from the core also puts a constraint on the graphite. The fuel salt must be excluded from the graphite to prevent local overheating and also to decrease fission-product poisoning, and this, in turn, requires that the graphite pore diameters not exceed one micron. This, however, is not a limitation, for the xenon removal will be shown below to require a gas permeability of the order of $10^{-8}$ cm$^2$/sec, and such a value requires pore diameters of $\sim 0.1\ \mu$.

Even though xenon is excluded from the graphite, it needs to be removed from the salt stream if the desired neutron economy is to be attained. This removal is accomplished by injecting helium bubbles into the flowing salt, which transfers the xenon from the salt to the bubbles and effectively removes xenon from the core region.

In the following sections we shall discuss in some detail: the method of analysis of existing data on radiation damage to permit prediction of the graphite lifetime in MSBR cores; the application of these damage rates and the radiation-induced creep to calculate induced stresses in the graphite; the considerations involved in the distribution and removal of $^{135}Xe$ and other noble gases; and last, the method proposed for safely

collecting and disposing of these gases. We conclude that graphite and the removal of xenon present no questions of feasibility, but require only minor extensions of existing technology.

## GRAPHITE LIFETIME

It has been recognized for several years that under prolonged radiation exposure, graphite begins to swell extensively, even to the point of cracking and breaking into fragments. However, data at high fluences and within the operating temperature ranges anticipated for molten-salt breeder reactors were largely nonexistent. Nevertheless, by using existing data, it was possible to estimate graphite behavior over the range of MSBR conditions. For a large group of commercial graphites—including British Gilso-graphite, Pile Grade A, and the American grades AGOT and CSF—it was found that the volume distortion, $\nu$, could be related to the fluence, $\Phi$, by a parabolic curve,

$$\nu = A\Phi + B\Phi^2 \quad , \tag{1}$$

where $A$ and $B$ are functions of temperature only. The fit of this equation to the experimental data is excellent for the isotropic Gilso-graphite, but the relation is approached only asymptotically for the anisotropic graphites. We may write the fluence as the product of flux and time, i.e., $\Phi = \phi t$. The behavior of $\nu$ is to decrease to a minimal value, $\nu_m$, and then increase, crossing the $\nu = 0$ axis at a defined time, $\tau$, given by

$$0 = A\phi\tau + B(\phi\tau)^2 \quad . \tag{2}$$

Clearly, in terms of $\nu_m$ and $\tau$, Eq. (1) can be rewritten as

$$\nu = 4\nu_m \frac{t}{\tau}\left(1 - \frac{t}{\tau}\right) \quad . \tag{2a}$$

For isotropic graphite, the linear dimensional changes will be given approximately by one-third the volume change. If the graphite is anisotropic, the preferred $c$-axis direction will expand more quickly, the other directions more slowly. This will induce a more rapid deterioration of the material in the preferred $c$-direction. As a consequence, we require that the graphite be isotropic, and can rewrite Eq. (2a) in terms of the linear distortion, $G$,

$$G = \frac{1}{3}\nu = \frac{4\nu_m}{3}\frac{t}{\tau}\left(1 - \frac{t}{\tau}\right) \tag{2b}$$

and this relation will be used hereafter.

The best values for the parameters $\phi\tau$ and $\nu_m$ were found to be

$$\phi\tau = (9.36 - 8.93 \times 10^{-3}\ T) \times 10^{22}\ \text{nvt}\ (E > \text{to keV})$$

and

$$\nu_m = -12.0 + 8.92 \times 10^{-3}\ T\ \% \quad ,$$

where $T$ is the temperature in °C, valid over the range 400 to 800°. At 700°C, these yield $\phi\tau = 3.1 \times 10^{22}$ with a 90% double-sided confidence limit of $\pm 0.2 \times 10^{22}$, and $\nu_m = -5.8\%$, with the limit ±0.2. Figure 1 shows the behavior of the linear distortion as a function of fluence with temperature as a parameter.

As pointed out in the introduction, it is necessary that the graphite exclude both salt and xenon. The first requires the graphite to have no pores larger than $\sim 1\,\mu$ in diameter; the second, as will be seen below, requires the graphite to have a permeability to xenon of the order of $10^{-8}$ cm$^2$/sec. Clearly, as the graphite expands and visible cracking occurs ($\nu > +3\%$), these requirements will have been lost. Lacking definitive data, we have made the *ad hoc* assumption that the pore size and permeability requirements will be maintained during irradiation until the time when the original graphite volume is reattained, namely, when $t = \tau$ as defined above.

To estimate the lifetime of an MSBR core, we must take into account the strong dependence of $\tau$

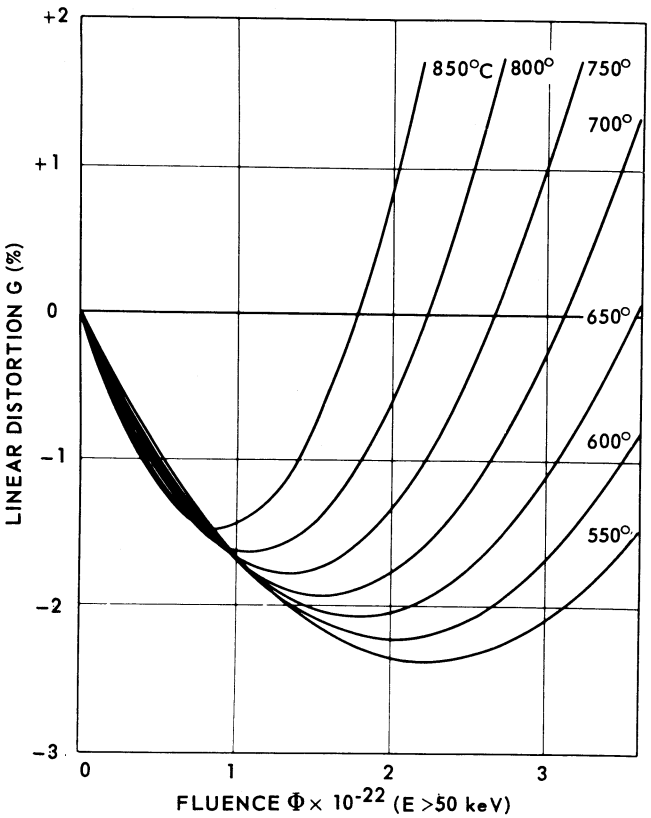


Fig. 1. Graphite linear distortion as a function of fluence at various temperatures.

on temperature, and the temperature of the core graphite will depend on the fuel salt temperatures, the heat transfer coefficient between salt and graphite, and the gamma, beta, and neutron heat generation in the graphite. In all core designs which have been analyzed, the power generation (i.e., fission rate) has been found to vary closely as $\sin(\pi z/l)$ along the axial centerline, where $z/l$ is the fractional height, and $l$ is the effective total core height. Thus, the heat generation rate in the graphite will vary as

$$q = q_0 + q_1 \sin(\pi z/l) \quad , \tag{3}$$

where $q_0$ approximates the rate due to delayed gamma, beta, and neutron heating, and $q_1$ approximates the maximum prompt heating. Representing the actual graphite core prisms as cylinders with internal radius $a$ and external radius $b$, we can readily calculate the internal temperature distribution assuming $q$ is not a function of radius. The result is[1]

$$T = T_a - \frac{q}{4K}(r^2 - a^2) + \frac{\log(r/a)}{\log(b/a)} \times \left[T_b - T_a + \frac{q}{4K}(b^2 - a^2)\right] \quad , \tag{4}$$

where $T_a$ and $T_b$ are the surface temperatures at $a$ and $b$, respectively, and $K$ the graphite thermal conductivity. Since the axial heat flow is negligible, the heat, $Q$, that must cross the graphite surfaces per unit area becomes

$$Q_a = -\frac{qa}{2} + \frac{K}{a \log b/a}\left[T_b - T_a + \frac{q}{4K}(b^2 - a^2)\right]$$
$$Q_b = -\frac{qb}{2} + \frac{K}{b \log b/a}\left[T_b - T_a + \frac{q}{4K}(b^2 - a^2)\right] \tag{5}$$

and if $h$ is the heat transfer coefficient between the salt and graphite interface, then also

$$Q_a = h(T_a - T_0)$$
$$Q_b = h(T_b - T_0) \quad , \tag{6}$$

where $T_0$ is the bulk salt temperature. The coefficient $h$ is calculated from the turbulent-flow Dittus-Boelter equation[2]

$$h = 0.023\ \mathrm{Re}^{0.8}\ \mathrm{Pr}^{0.4}\frac{K_0}{2a} \quad , \tag{7}$$

where

Re is the Reynolds number

Pr is the Prandtl number

$K_0$ is the salt thermal conductivity.

We are assuming the coolant channels at the outer surfaces of the cylinder will have the same effective hydraulic radius as the interior channel of radius $a$. Finally, since the heat capacity of the salt is a weak function of temperature, in keeping with the sinusoidal variation of power density along the axis, the salt temperature, $T_0$, becomes

$$T_0 = \frac{1}{2}\left[T_f + T_i - (T_f - T_i)\cos\frac{\pi z}{l}\right] \tag{8}$$

in which $T_i$ and $T_f$ are the entering and exiting temperatures, respectively, of the salt.

Equations (3) through (8) completely determine the temperatures in the graphite. As we shall see below, the radiation-induced strain in the graphite along the $z$-axis, i.e., $\Delta z/z$, is given by

$$\frac{\Delta z}{z} = \frac{2}{(b^2 - a^2)}\int_a^b G(T)\, r\, dr \quad ,$$

where $G(T)$ is the damage function of Eq. (2b). A similar expression applies to the radial strain. A negligible error is introduced by approximating the right-hand side by $G(\overline{T})$, where $\overline{T}$ is the average temperature over the cross section; therefore,

$$\frac{\Delta z}{z} = G(\overline{T}) \quad . \tag{9}$$

Since $\overline{T}$ varies with $z/l$, each point along the cylinder will have a different life, $\tau(\overline{T})$, defined by $\Delta z/z = 0$. The minimum value of these $\tau(\overline{T})$ thus defines the time at which the cylindrical prism should be replaced based on our criterion.

The properties of the fuel salt and graphite which are required in the above equations are given in Table I. The graphite is assumed to be similar to the British Gilso-graphite, although there are other coke sources than Gilsonite which lead to isotropic materials.

Calculations have been made on two core configurations. Case No. CC-58 is the reference design discussed elsewhere[3] in this series of

TABLE I

Materials Properties Used in Graphite Lifetime and Stress Calculations

| | |
|---|---|
| **Fuel Salt** | |
| Thermal conductivity, W/(cm °C) | $1.29 \times 10^{-2}$ |
| Specific heat, W sec/(g °C) | 1.36 |
| Viscosity, cP | $(7.99 \times 10^{-2})\ \exp(4342/T\ °K)$ |
| **Graphite** | |
| Thermal conductivity, W/(cm °C) | $37.63\ \exp(-0.7T\ °K)$ |
| Thermal expansion, $(°C)^{-1}$ | $5.52 \times 10^{-6} + 1.0 \times 10^{9}(T\ °C)$ |
| Young's modulus, psi | $1.9 \times 10^{6}$ |
| Poisson's ratio | 0.27 |
| Creep constant, $k$ | $(5.3 - 1.45 \times 10^{-2}T + 1.4 \times 10^{-5}T^2) \times 10^{-27}$ |
| | $k$ in $\mathrm{psi}^{-1}$ n/(cm² sec) |
| | T in °C. |

papers. This design optimizes the fuel conservation coefficient[4] with the peak power density constrained to a value of 63 W/cm$^3$ to prolong graphite life. Case No. CC-24 is the identical core scaled to a smaller geometry (half the volume of No. CC-58) and with the constraint on graphite lifetime raised. In both cases the fuel conservation coefficient is 15.1 [MW(th)/kg][2]. The damaging flux in case No. CC-24 is also more typical of the case when the core is optimized with no constraints. The pertinent core parameters[4] are given in Table II.

TABLE II

Relevant Core Characteristics for Calculation of Graphite Lifetime and Stresses

| | Case No. CC-24 | Case No. CC-58 |
|---|---|---|
| Peak flux ($E \geq 50$ keV), n/(cm$^2$ sec) | $5.15 \times 10^{14}$ | $3.2 \times 10^{14}$ |
| Salt flow per unit area, g/(cm$^2$ sec) | $1.39 \times 10^3$ | $8.21 \times 10^2$ |
| Heat generation, delayed, W/cm$^3$ | 1.16 | 0.71 |
| Heat generation, prompt, W/cm$^3$ | 7.17 | 4.39 |
| Salt inlet temperature, °C | 550 | 550 |
| Salt outlet temperature, °C | 700 | 700 |

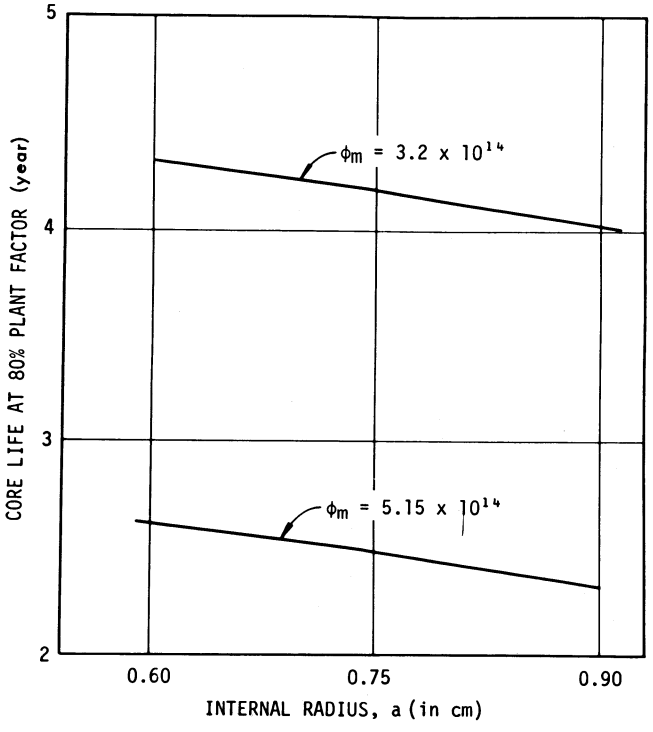


Fig. 2. Core lifetime as a function of graphite prism dimensions for cores with peak damage fluxes of 3.2 and 5.15 $\times$ $10^{14}$ nv ($E$ > 50 keV). In all cases the ratio of the radii, $b/a$, is 6.67.

Since the salt-to-graphite ratios in the core are determined by nuclear requirements, and the salt flow by cooling requirements, the only variable left at this point is the absolute value of the internal radius $a$, which scales the size of the graphite prisms. Figure 2 shows the lifetime of the central graphite prism as it is affected by the radius $a$; there is an obvious decrease in core life as the radius $a$ increases and the internal graphite temperatures climb. We note that the ratio of fluxes in the two cases is 1.61; at $a$ = 0.9 cm, the corresponding reciprocal ratio of lifetimes is 1.74, the additional gain in lifetime at the lower flux being due to decreasing graphite temperatures.

The latter case has been studied in more detail since it corresponds to the current reference design concept. For this design the equivalent radii are

$$a = 0.762 \text{ cm}$$

$$b = 5.39 \text{ cm} .$$

The associated temperature distributions for the central core prisms are given in Fig. 3, and the local lifetimes $\tau(\bar{T})$ as a function of $z/l$ in Fig. 4. The life of the prism, i.e., the minimal $\tau(\bar{T})$, occurs at $z/l$ = 0.55 and has a value of 4.1 years at 80% plant factor. The entire prism will change length as given by the integral of the right-hand side of Eq. (9) over the length of the prism; this is shown as a function of time in Fig. 5. The radial distortion for various times is shown in Fig. 6, and gives the prism a double hourglass shape toward the end of life.

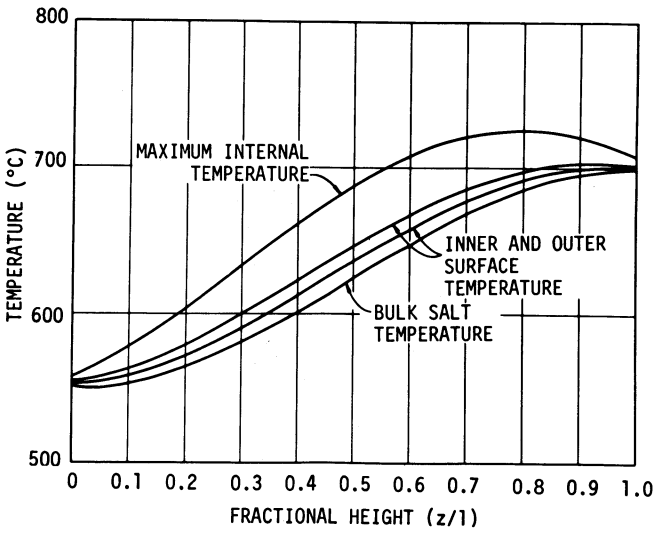


Fig. 3. Temperatures associated with the central graphite prism as a function of vertical position for the reference core design.

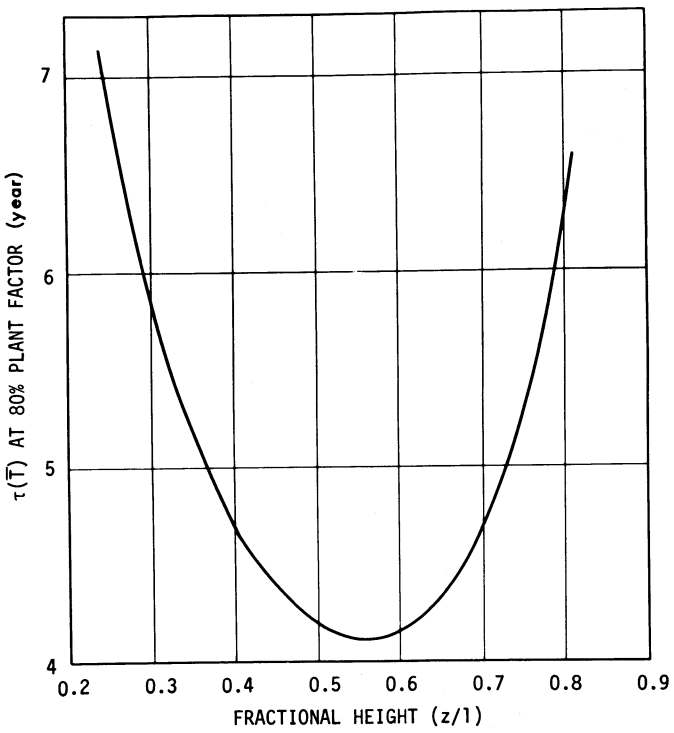


Fig. 4. Local lifetime $\tau(\overline{T})$ as a function of vertical position for the central graphite prism of the reference core design.

The cost of replacing graphite will include both material procurement and labor. We have estimated these costs based on an industry supplying the order of ten or more reactors. The total operating cost associated with graphite replacement would amount to ~0.2 mill/kWh for a two-year life, or 0.10 mill/kWh for a four-year life. (Capital investment would also be required for the replacement equipment and is included in the capital cost estimates of Bettis and Robertson.[3]) Thus, the cost penalty associated with graphite replacement is not a crippling one, although it is large enough to merit considerable effort on graphite improvement.

Assuming pyrolytic impregnation, as discussed by McCoy et al.,[5] successfully excludes xenon from the graphite, three significant material requirements need to be met: the graphite must be isotropic, have entrance pore diameters $<1\ \mu$, and have a radiation stability at least as good as the Gilso-graphite. All of these requirements can be met with existing graphite technology, although all have not been met in a single graphite of the dimensions required. Unquestionably, there will be production difficulties in initially producing such a graphite, but the problems will be in process control rather than in basic technology.

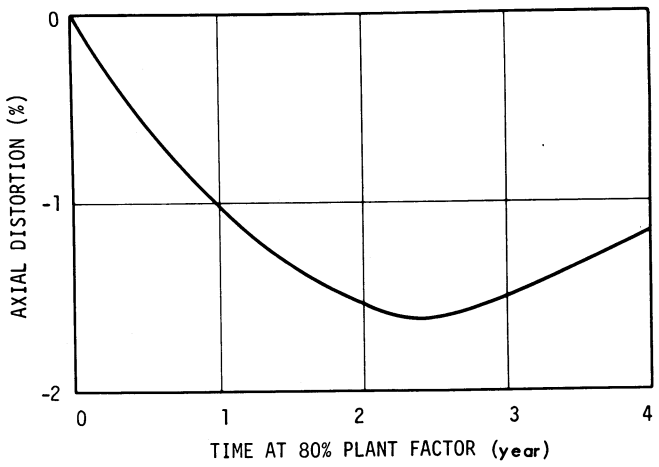


Fig. 5. Axial distortion of the central graphite prism as a function of time for the reference design.

## INTERNAL STRESSES IN THE GRAPHITE

In the preceding section we have tacitly assumed that the thermal and radiation-induced stresses developed during the lifetime of the graphite are not limiting. We turn now to validate this assumption. We again consider the central prism as in the preceding section, and have for the constitutive equations,

$$\dot{\epsilon}_i = \frac{1}{E}\left[\dot{\sigma}_i - \mu(\dot{\sigma}_j + \dot{\sigma}_k)\right] + k\phi\left[\sigma_i - \frac{1}{2}(\sigma_j + \sigma_k)\right] + g\ , \tag{10}$$

where

$\epsilon_i$ = strain in the $i$'th direction

$\sigma_i$ = stress

$E$ = Young's modulus

$\mu$ = Poisson's ratio

$k$ = secondary creep constant

$\phi$ = damaging flux

dots = time derivatives

$g = dG/dt$ = damage rate function defined from Eq. (2b).

In cylindrical coordinates, $i = (r, \theta, z)$. In the absence of externally applied stresses and because of the vanishing of $\phi$ at the ends of the core prism, the $z$ component of strain will not be a function of $r$ and $\theta$ (plane strain). We shall assume $k$ is a function of $\overline{T}$, but will not let $k$ or $\phi$ vary with $r$ and $\theta$. Then Eq. (10) can be integrated in closed form. The resulting dimensional changes in the prism are

$$\frac{\Delta z}{z} = \frac{\Delta a}{a} = \frac{\Delta b}{b} = \overline{G}\ , \tag{11}$$

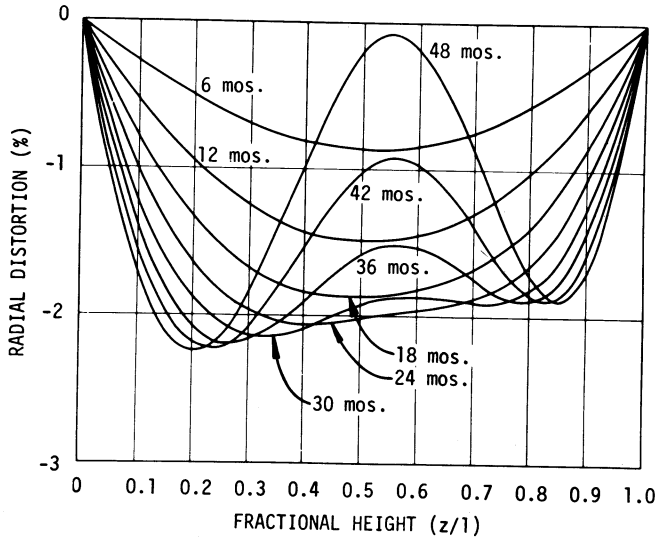


Fig. 6. Radial distortion of the central graphite prism as a function of vertical height for the reference design. Times are calculated at 80% plant factor.

where $\bar{G}$ is the average value of $G$ over the cylindrical cross section. Hence the prism behaves locally as though it were at the average radiation distortion $\bar{G}$.

The tensile stresses are maximum at the outside surface of the cylinder, and are given by

$$\sigma_r(b) = 0, \quad \sigma_\theta(b) = \sigma_z(b)$$

and

$$\sigma_z = \frac{E}{1-\mu} e^{-\beta t} \int_0^t [\bar{g} - g(r)] e^{\beta t} dt + \sigma_{z0} e^{-\beta t} \quad (12)$$

with

$$\beta = \frac{Ek\phi}{2(1-\mu)} .$$

We may consider the initial stress $\sigma_{z0}$ to be the thermal stresses introduced as the reactor is brought to power, and these anneal out exponentially with time because of the radiation-induced creep. We are interested only in large times $t$, and if we set

$$\Delta g = \bar{g} - g(b)$$

and remember $g$ is a linear function of time

$$g = \frac{dG}{dt} = \frac{4}{3}\frac{\nu_m}{\tau}\left(1 - \frac{2t}{\tau}\right) = g_0 + g_1 t ,$$

then

$$\Delta g = \Delta g_0 + \Delta g_1 t$$

and Eq. (12) thus takes the asymptotic form

$$\sigma_z \rightarrow \frac{2}{k\phi}(\Delta g_0 - \beta \Delta g_1) + \frac{2}{k\phi}\Delta g_1 t . \quad (13)$$

It can also be shown that $\bar{g} = g(\bar{T})$ with an error not exceeding 2% for the parameter values of interest.

The thermal stresses have the same interrelationships as the radiation stresses, and are given by

$$\sigma_{r0}(b) = 0, \quad \sigma_{\theta 0}(b) = \sigma_{z0}(b)$$

and

$$\sigma_{z0} = \frac{\alpha E}{1-\mu}[\bar{T} - T(r)] e^{-\beta t} . \quad (14)$$

We may substitute this result into Eq. (12) to give the maximum stress $\sigma_z(b)$ throughout the entire life of the central prism.

For the reference design concept, the maximum stresses also occur at the point $z/l = 0.55$ and are shown in Fig. 7. The stresses reach a maximum at the end of life and amount to only 490 psi. Since the isotropic graphite which is presumably to be used in the reference design would have a tensile strength in the range 4000 to

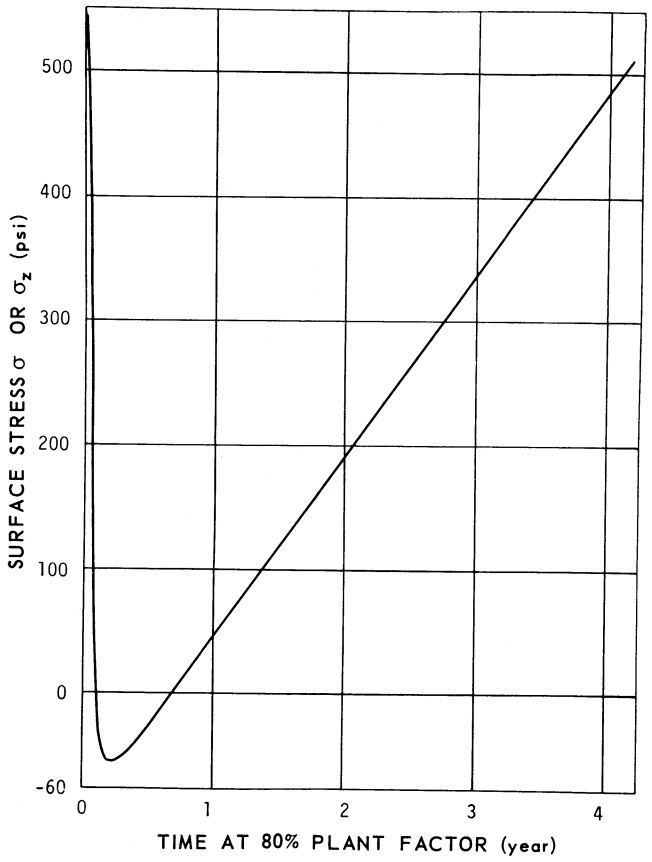


Fig. 7. Axial or tangential surface stress at $z/l = 0.55$ as a function of time.